

EMERGENCE AND EVOLUTION OF PATTERNS

Harry L. Swinney

Center for Nonlinear Dynamics and Department of Physics
University of Texas, Austin, TX 78712 USA
(swinney@chaos.ph.utexas.edu)

Abstract. We consider macroscopic systems driven away from thermodynamic equilibrium by an imposed gradient in temperature, velocity, or concentration. For a sufficiently small imposed gradient, a system will assume (asymptotically) the symmetry of the boundary conditions. However, when the imposed gradient exceeds a critical value, a system will spontaneously break the symmetry of the boundary conditions and form a spatial pattern. In two dimensions the pattern could be traveling waves (e.g., spirals) or an array of squares, stripes, or hexagons. With larger imposed gradients, the patterns can become more complex and even disordered in both space and time. We discuss the general principles of pattern formation in systems driven away from equilibrium and illustrate the principles with examples from experiments.

NEAR EQUILIBRIUM: THE BASE STATE

We consider macroscopic systems such as fluids, liquid crystals, reacting chemical liquids or gases, solids, and biological systems, which are driven away from thermodynamic equilibrium. The systems are *dissipative* — energy must be supplied through the imposition of a gradient (e.g., in temperature, velocity, or concentration) to maintain the system away from equilibrium. The distance away from equilibrium can often be characterized by one or more dimensionless control parameters, e.g., the Reynolds number for a fluid, $R = VL/\nu$ for a fluid flow with a characteristic velocity V , length scale L , and kinematic viscosity ν .

The dynamical behavior of macroscopic systems driven away from thermodynamic equilibrium is usually governed by partial differential equations. Again taking a fluid as an example, the equation of motion for the velocity field $\mathbf{u}(\mathbf{r}, t)$ and the pressure field $p(\mathbf{r}, t)$ is the Navier-Stokes equation,

$$\frac{\partial \mathbf{u}}{\partial t} + (\mathbf{u} \cdot \nabla) \mathbf{u} = -\nabla p + \frac{1}{R} \nabla^2 \mathbf{u}, \quad (1)$$

which is Newton's second law for a continuum fluid. For an incompressible fluid, we also have

CP501, *Stochastic Dynamics and Pattern Formation in Biological and Complex Systems*,
edited by S. Kim, K. J. Lee, and W. Sung
2000 American Institute of Physics 1-56396-914-9

$$\nabla \cdot \mathbf{u} = 0. \quad (2)$$

Equations (1) and (2) are dimensionless — \mathbf{u} , \mathbf{r} , t , and p are expressed in units of V , L , L/V , and ρV^2 . Thus two systems with the same geometry but with a different size, velocity scale, and viscosity will behave in the same way if the Reynolds numbers are the same.

Even when a system is driven so far from equilibrium that the behavior becomes chaotic or turbulent, varying erratically in space and time, the system is still usually completely described by deterministic equations of motion such as (1), i.e., stochastic effects such as thermal fluctuations are usually negligible.

The solution of the nonlinear equation of motion near equilibrium is called the *base state*. For simple geometries the base state can usually be determined analytically, while for complicated geometries the base state must be determined numerically. The base state has the symmetry of the boundary conditions; hence for time-independent boundary conditions, the base state is time independent. Sufficiently close to equilibrium, the base state is stable — any perturbation, no matter how large, will decay and the system will asymptotically approach the base state. For sufficiently small R , *any* initial condition will evolve to the base state; in contrast, for large R , the uniqueness property is lost, and there may be several or even many different stable solutions for a given R .

INSTABILITY OF THE BASE STATE

We now consider the linear stability of the base state solution $\mathbf{u}(\mathbf{r}, t)$. If an infinitesimal perturbation of the base state, $\delta\mathbf{u}(\mathbf{r}, t) = \mathbf{A}e^{\sigma t}e^{i\mathbf{k}\cdot\mathbf{r}}$, decays, then the base state is stable with respect to small perturbations. As the distance away from equilibrium increases, a critical value of R , R_c , is reached where the growth rate of the perturbation is zero at a wavenumber k_c , and for $R > R_c$, the perturbation grows, as Fig. 1(a) illustrates. R_c can be found by solving the equation of motion, linearized in $\delta\mathbf{u}$. The base state loses stability at R_c and the solution spontaneously loses the symmetry of the boundary conditions — perturbations at wavenumber k_c grow, developing into a spatial pattern with wavelength $\lambda = 2\pi/k_c$.

In 1923, G. I. Taylor conducted a linear stability analysis of flow between concentric rotating cylinders [1]. The base state for this system is an axisymmetric velocity field that is invariant under translation in the axial direction. Only the azimuthal component of the velocity is nonzero, $u_\theta = Ar + B/r$, where the constants A and B are determined by the no-slip boundary conditions at the inner and outer cylinders, $u_\theta(r_1) = \Omega_1 r_1$ and $u_\theta(r_2) = \Omega_2 r_2$, where the subscripts 1 and 2 correspond to the inner and outer cylinders, respectively. Taylor calculated the critical values of the cylinder rotation rates (Ω_1 , Ω_2) where the base state becomes unstable. Taylor also built a concentric cylinder apparatus and used dye to visualize the flow patterns that form at the critical rotation rates. He observed that beyond the onset of the instability, axisymmetric toroidal vortices form, encircling

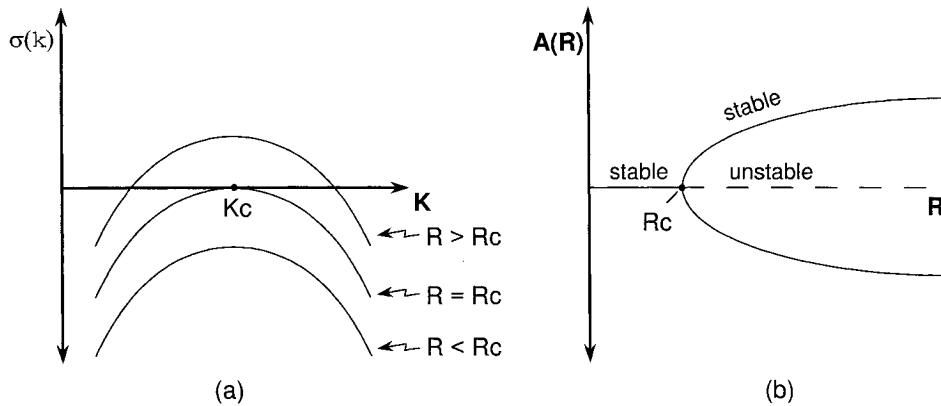


FIGURE 1. (a) Growth rate of a perturbation, $\sigma(k)$, as a function of wavenumber for Reynolds numbers below, at, and above the onset of instability. (b) The amplitude of the mode that becomes unstable at $R = R_c$. The transition at R_c is called a pitchfork bifurcation. The base state remains a solution of the equation of motion for $R > R_c$, but it is no longer stable.

the inner cylinder. The vortices are stacked like a pile of doughnuts in the axial direction; at a boundary between one vortex pair, fluid flows inward towards the inner cylinder, while at the next boundary in either axial direction, fluid flows outward towards the outer cylinder. The observed wavelength of a pair of vortices agreed well with the value calculated from the linear stability analysis. Moreover, Taylor found remarkable agreement between the predictions of the stability analysis and the laboratory observations, as Fig. 2 shows. This was the first experimental test of a linear stability analysis for any system driven away from equilibrium. As Taylor said, “All [previous] attempts to calculate the speed at which any type of flow would become unstable have failed” [1].

The procedure for finding the instability of the base state is straightforward, but in practice there can be subtleties in both experiments and in analyses. For example, one of the earliest instabilities studied in experiments was a thin layer of fluid heated from below. Nearly a century ago Henri Bénard [2] discovered that hexagonal convection cells form at a well-defined threshold; one of Bénard’s photographs is shown in Fig. 3(a). In 1916, Rayleigh conducted a linear stability analysis for the problem, assuming that buoyancy effects caused the convection, but the threshold that Rayleigh predicted did not agree with Bénard’s observations [3] (note that Rayleigh’s analysis of convection preceded Taylor’s analysis of flow between cylinders). Forty years elapsed before it was recognized that the instability observed by Bénard was not caused by buoyancy but by surface tension gradients [4]. Even then, experiments remained in disagreement with theory until recently, when the experimental difficulties were finally resolved; the observations shown in Fig. 3(b) are in good accord with theory [5].

When the growth rate of a perturbation, σ (Eq. (3)), is complex rather than

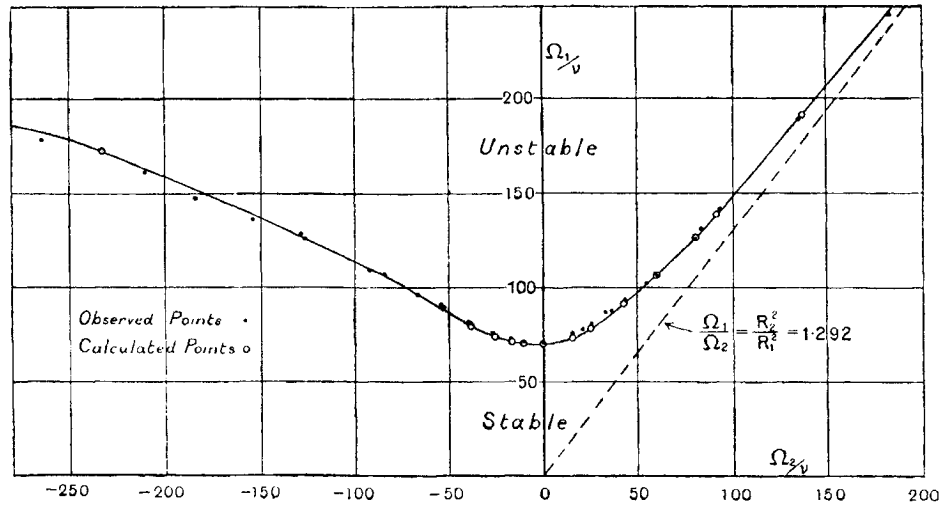


FIGURE 2. G.I. Taylor's stability diagram for flow between concentric cylinders with the inner cylinder rotating with angular velocity Ω_1 and the outer cylinder rotating with angular velocity Ω_2 . The solid dots are Taylor's measurements and the open circles are from Taylor's linear stability analysis. The cylinders are co-rotating in the right-hand quadrant and counter-rotating in the left-hand quadrant; 0 corresponds to thermodynamic equilibrium. Reprinted with permission from the Phil. Trans. Roy. Soc. [1].

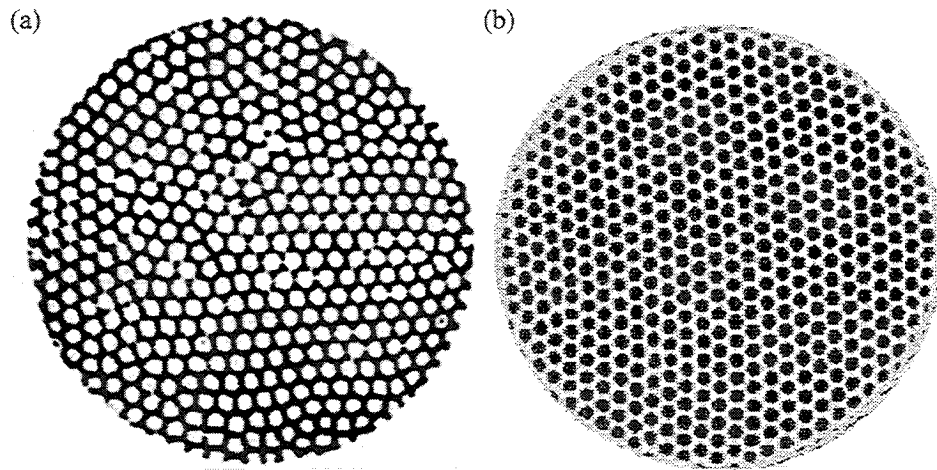


FIGURE 3. Hexagonal convection patterns observed in thin liquid layers heated from below: (a) Bénard (1900) [2] and (b) Schatz et al. (1995) [5].

real, instability of the uniform state leads to an oscillatory rather than stationary secondary state. The pattern that forms at the instability often consists of traveling waves in the form of spirals. Rotating spirals were observed in a chemical reaction-diffusion system more than two decades ago. The chemical reagents were poured into a petri dish, and a pattern with many rotating spirals formed and evolved as the chemicals were consumed [6]. Spiral wave patterns have also been observed in convecting fluids [7], *Xenopus* oocytes (the spirals in these frog eggs are waves of calcium concentration) [8], heterogeneous catalysis [9], and even heart muscle [10] (where the interest is motivated by a possible connection with sudden cardiac death [11,12]).

A linear stability analysis yields the critical parameter value at which a base state becomes unstable, but perturbation theory must be used to determine how the amplitude A of the the most unstable mode (the mode with wavenumber k_c) varies above the instability threshold. In the simplest cases it is sufficient to truncate the amplitude expansion at cubic order,

$$\frac{dA}{dt} = \sigma A + bA^3, \quad (3)$$

where the quadratic term is absent because the cubic term is the lowest order term that feeds back on the unstable mode. Expanding the coefficients about R_c , we have

$$\sigma(R) = \sigma_0 + \sigma_1(R - R_c) + \dots, \quad (4)$$

$$b(R) = b_0 + b_1(R - R_c) + \dots. \quad (5)$$

Since $\sigma(R_c) = \sigma_0 = 0$,

$$\frac{dA}{dt} = \sigma_1(R - R_c)A + b_0A^3, \quad (6)$$

where $b_0 < 0$ for stability (for $b_0 > 0$, higher order terms would be needed for stability), and $\sigma_1 > 0$ since the system is unstable for $R > R_c$. The steady state amplitude, $dA/dt = 0$, is given by

$$A \propto \sqrt{R - R_c}. \quad (7)$$

The square-root growth in the amplitude of the secondary state is illustrated in Fig. 1(b). This square-root growth of the amplitude has been confirmed in many experiments, e.g., for Taylor vortex flow, see [13].

Beyond the threshold of instability there is a band of unstable wavenumbers (cf. Fig. 1(a)) and the amplitude $A(\mathbf{r}, t)$ of the pattern can vary slowly in space and time. For a given type of instability, there is universal form for the equation describing the amplitude near threshold. For example, a pattern of two-dimensional

stationary rolls (also called stripes) that emerges at an instability from a uniform state is governed by

$$\tau_0 \frac{\partial A}{\partial t} = \frac{R - R_c}{R_c} A + \xi_0^2 \left(\frac{\partial}{\partial x} - \frac{i}{2k_c} \frac{\partial^2}{\partial y^2} \right) A - g_0 |A|^2 A, \quad (8)$$

where the constants τ_0 , ξ_0 , k_c , and g_0 depend on the detailed properties of individual systems [14]; in principle these constants can be derived from the equations of motion, but this has been done for only a few cases. Much has been learned from comparison of predictions of amplitude equations with experiments (see especially the work on Rayleigh-Bénard convection, that is, fluid convection in a box heated from below [15]).

The possibility that instability could lead to the spontaneous formation of spatial patterns in chemical systems was first proposed in 1952 by Alan Turing in a paper entitled “The Chemical Basis of Morphogenesis” [16]. Turing considered systems of reaction and diffusing chemical species, governed by

$$\frac{\partial \mathbf{c}}{\partial t} = \mathbf{D} \nabla^2 \mathbf{c} + \mathbf{f}_\mu(\mathbf{c}), \quad (9)$$

where $\mathbf{c}(\mathbf{r}, t)$ is a vector of concentrations of different species, \mathbf{D} is the diffusion coefficient matrix, \mathbf{f} is a function describing the chemical kinetics (nonlinear in the cases of interest), and μ represents the control parameters (e.g., reagent concentrations, temperature) [17]. Turing said, “Such a system, although it may originally be quite homogeneous, may later develop a pattern or structure due to an instability of the homogeneous equilibrium.” Turing’s analysis stimulated considerable theoretical research on mathematical models of pattern formation in chemical and biological systems (e.g., see [18]), but Turing-type patterns were not observed in controlled laboratory experiments until 1990 [19]. The absence of experiments was due to a lack of a device in which a reaction-diffusion system could be maintained in well-defined nonequilibrium conditions. Such a device was developed in the late 1980s [20–23]. It is simply a thin gel layer with its surfaces in contact with well-stirred reservoirs that are continuously refreshed. This type of reactor was used to observe the Turing patterns shown in Fig. 4 [22]. As a control parameter (reagent concentration or temperature) was varied, a critical value was reached where there was a spontaneous transition from a uniform (nonpatterned state) to the hexagonal pattern shown in Fig. 4(a). At other reagent concentrations, patterns of stripes rather than hexagons form; see Fig. 4(b).

What sets the length scale in the patterns in nonequilibrium systems? The size of the lattice constant in a crystalline lattice is determined by the atomic potential, but the length scales in patterns such as in Figs. 3 and 4 are many times larger. In fluid patterns the length scale is determined by the geometry. For example, a toroidal Taylor vortex near the onset of instability in flow between concentric rotating cylinders has an axial length very nearly equal to the gap between the cylinders. For chemical patterns the wavelength λ is determined not by the geometry but by the intrinsic properties of the reaction-diffusion system: $\lambda \propto \sqrt{D\tau}$,

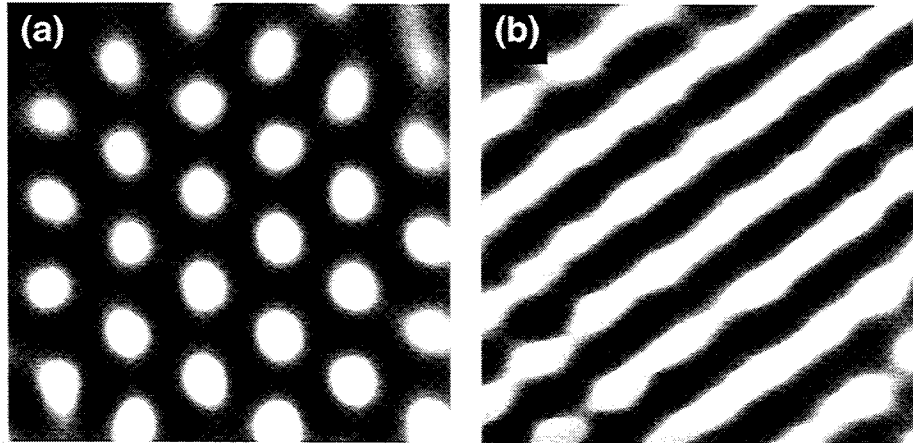


FIGURE 4. (a) Hexagonal and (b) stripe patterns of chemical concentration that form spontaneously in a continuously fed laboratory thin gel reactor. The darker regions represent higher concentrations of triiodide, which is one of the species in the reaction. Each image is 1 mm \times 1 mm. Reprinted by permission from Nature [<http://www.nature.com>], copyright 1994, Macmillan Magazines Ltd. [22].

where D and τ are a characteristic diffusion coefficient and time scale (e.g., a period of an oscillation of the homogeneous reaction) [23].

Bifurcations from a spatially uniform state to stationary arrays of hexagons, stripes, and squares have been observed in many systems, e.g., hexagonal arrays like those in Figs. 3 and 4 have recently been observed in an optical beam in a nonlinear medium [24] and in a gas of electrons in a strong magnetic field [25]. Another example is shown in Fig. 5: a vertically oscillated layer of liquid spontaneously forms stationary surface wave patterns when the acceleration amplitude exceeds a critical value; the patterns at the onset of instability can be squares or stripes, as Fig. 5 illustrates.

FAR BEYOND THE ONSET OF INSTABILITY: EXPERIMENTS, SIMULATIONS, AND SYMMETRY

Perturbation theory provides a satisfactory description of the transition from a uniform state to spatial patterns in systems driven away from equilibrium, as described in the previous section. However, at control parameter values far beyond that at which the base state becomes unstable, perturbation theory fails. Experiments and numerical simulations reveal (for increasing R or other relevant control parameters) secondary and higher instabilities, each of which leads to a spatiotemporal pattern that breaks a space and/or time symmetry of the previous state. This

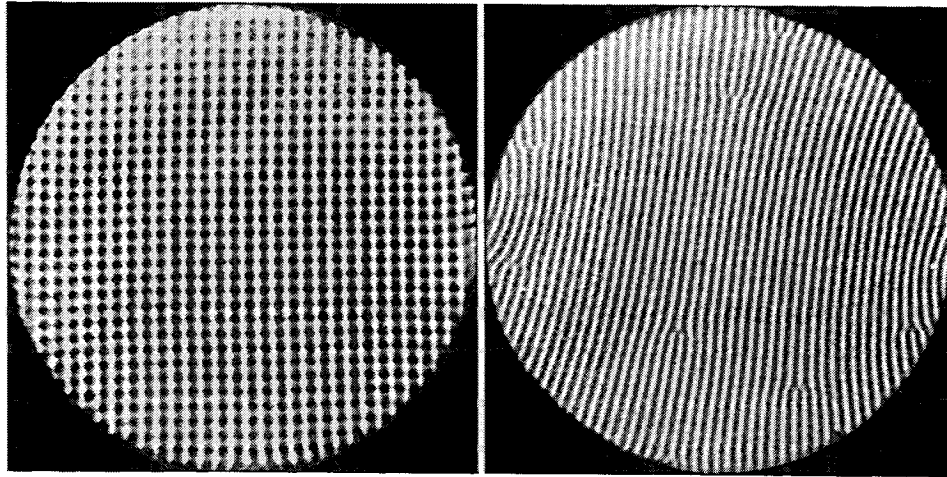


FIGURE 5. (a) Square and (b) stripe standing wave patterns in a vertically oscillated layer of liquid just below the liquid-vapor critical point; (a) is at $0.08K$ below the critical temperature and (b) is at $0.02K$ below the critical temperature [26]. The cell diameter is 10 mm, the container oscillation frequency is 60 Hz, and the fluid is carbon dioxide.

cascade of instabilities often leads ultimately to states that are disordered in both space and time, even turbulent.

There is no general theory to describe the behavior of systems far beyond primary instability. In contrast to equilibrium systems, there is no function like the free energy that can be determined and minimized to find the state of a nonequilibrium system for a given set of control parameters. The many attempts to find an extremum principle for systems far from equilibrium have all failed. However, it is just this regime far from equilibrium that is often of interest in nature and technology, where one would like to be able to predict the behavior of, e.g., the atmosphere and oceans (weather and climate), combustion, mixing and separation processes, and biological systems.

In the absence of a general theory, experiments and simulations provide a guide to the kinds of phenomena that can occur. Figure 6 is an experimentally determined phase diagram showing the instabilities observed in flow between independently rotating cylinders [27]. The curve marking the primary instability (the lowest curve) is the one determined by Taylor (cf. Fig. 2).

Very little is understood about the different regimes shown in Fig. 6, especially those well beyond the primary instability. But one might argue that since we know the equation of motion, the problem is really solved. This is not true. The Navier-Stokes equation has been known for more than a century, but, despite a century of theoretical interest in flow between concentric cylinders, there was no hint of the complex phase diagram shown in Fig. 6 until it was determined in experiments. Thus knowledge of the equations of motion is not enough. Freeman Dyson recently

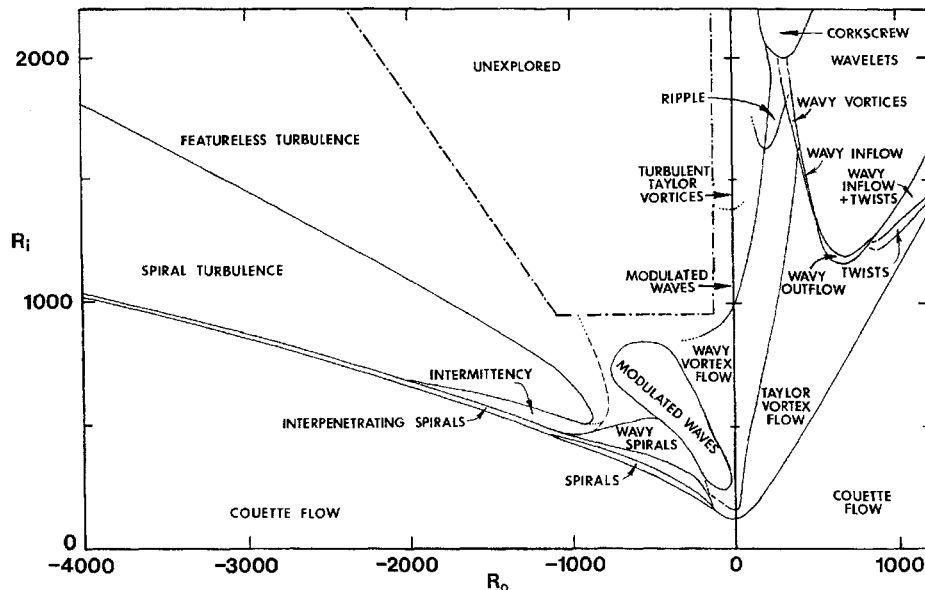


FIGURE 6. Regimes observed in flow between concentric independently rotating cylinders. R_i and R_o are Reynolds numbers proportional to the rotation rates of the inner and outer cylinders respectively. The phase diagram is different for cylinders of different radius ratios; this diagram is for cylinders with radius ratio 7/8. Reprinted with permission from *J. Fluid Mech.*, Cambridge University Press [27].

made this point [28]:

Oppenheimer in his later years believed that the only problem worthy of the attention of a serious theoretical physicist was the discovery of the fundamental equations of physics. Einstein certainly felt the same way. To discover the right equations was all that mattered. Once you had discovered the right equations, then the study of particular solutions of the equations would be a routine exercise for second-rate physicists or graduate students. ... It often happens that the understanding of the mathematical nature of an equation is impossible without a detailed understanding of its solutions. The black hole is a case in point. One could say without exaggeration that Einstein's equations of general relativity were understood only at a very superficial level before the discovery of the black hole.

One could even go further — knowledge of the solutions of the equations of motion may not be enough. Philip Holmes found this was the case in his analysis of the constrained Euler buckling problem [29]. The solution he obtained, involving

pages of elliptic integrals, did not provide much insight. The bifurcation structure for this problem was not understood until the bifurcations were identified in numerical simulations; then the mathematical solution could be examined to determine the behavior in the neighborhood of each bifurcation. Holmes' point is that experiments or simulations are often still needed, even when a closed form solution is known.

Experiments and numerical simulations of models help in understanding the kinds of bifurcations and patterns that can occur far from equilibrium. By "models" we mean systems of nonlinear partial differential equations that are simpler and hence easier to explore numerically and analytically than the full equations of motion (e.g., the Navier-Stokes equation). Amplitude equations such as Eq. (8) become models (often called complex Ginzburg-Landau models) when studied beyond the range where perturbation theory is applicable. Two other models that have been widely studied are the Swift-Hohenberg equation and the Kuramoto-Sivashinsky equation [14].

Figure 7 shows a phenomenon that, after it was observed in a laboratory experiment, led to the kind of interplay between model studies and laboratory experiments that is typical in investigations of nonequilibrium systems. The figure illustrates the development of a transverse instability of a chemical front. The instability was discovered in a search for Turing patterns in experiments on a reaction-diffusion system that had not been previously studied [30]. Several reaction-diffusion models with two species were then examined to search for a similar front instability. The laboratory reaction is much more complex than the two species models; five chemical species are fed to the laboratory reactor, and the reaction produces many intermediate species and reaction products. However, each of the studies of models with only two species yielded a front instability similar to that illustrated by Fig. 7 [31–34].

One of the simulations that yielded a front instability revealed another phenomenon that had not been seen in the experiments: patterns of spots (domains with a chemical concentration different from the background) that undergo a continuous process of "birth" through replication and "death" through overcrowding [33]. A search for this phenomenon in laboratory experiments was successful, as Fig. 8 shows. Moreover, the experiments show that if a spot is isolated, it grows until the center drops back into the low pH state, thus forming a doughnut-like pattern. A subsequent study revealed this behavior in the numerical simulations as well. Front instabilities are common in systems far from equilibrium, but further experiments, simulations, and analyses are needed to determine what general lessons can be gleaned from the studies of the chemical fronts shown in Figs. 7 and 8.

An analysis of the consequence of symmetries can lead to insights into particular instabilities and to general insights on pattern formation [36]. An example of use of symmetry to analyze the stability of a particular flow is a study by Iooss [37], who considered what symmetries would be possible for secondary flows that bifurcate from Taylor vortex flow, given the possible axial reflection and translation

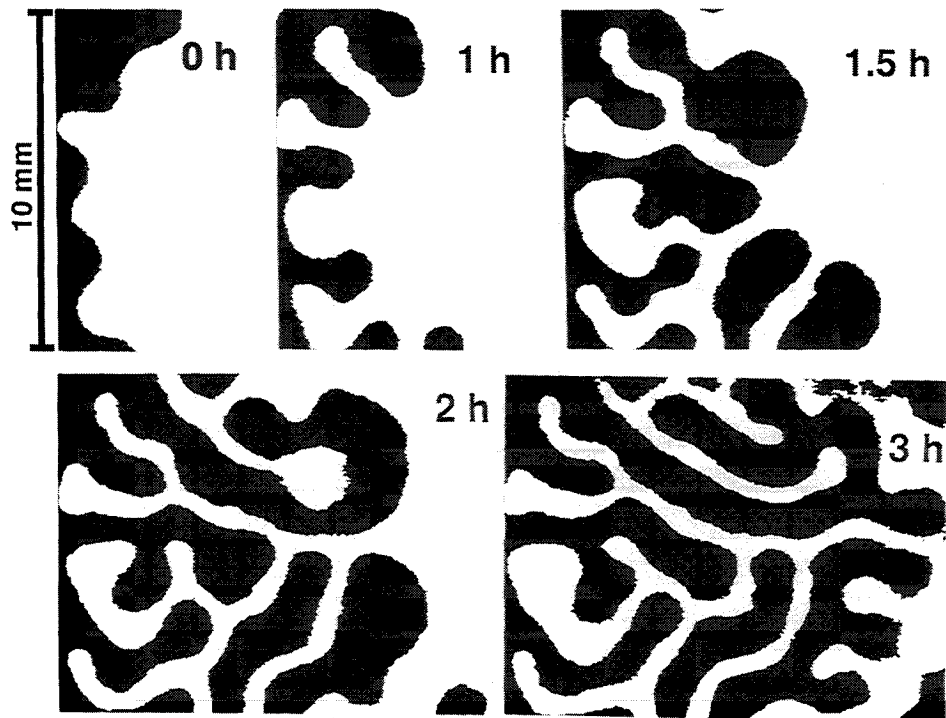


FIGURE 7. Time evolution of pattern observed in a bistable reaction-diffusion system (a ferrocyanide-iodate-sulfite reaction). The white state has low pH (about 4) and the black state has high pH (about 7). There is a transverse instability of the front that separates the black and white states, and the front evolves until at 3 hours (last picture) a stable, stationary labyrinthine pattern is achieved. Reprinted with permission from Science, copyright 1993, American Association for the Advancement of Science [30].

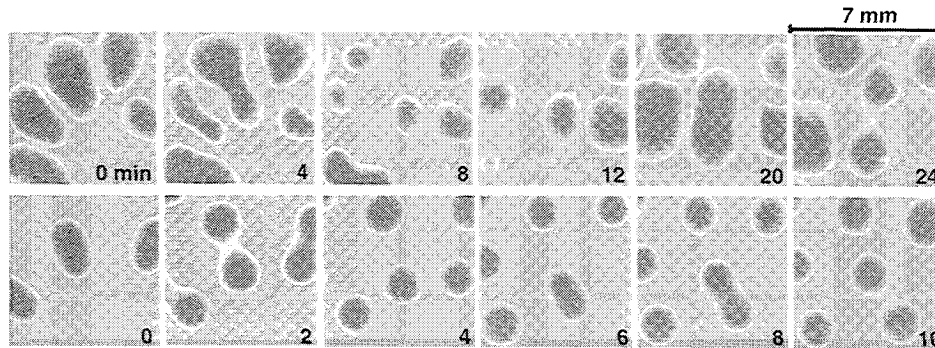


FIGURE 8. Replicating spot patterns in a laboratory experiment (upper row) and in a numerical simulation of a two-species model (lower row). In the experiment, the darker regions have higher pH (about 7) than the lighter regions (about pH 3). Reprinted by permission from Nature [<http://www.nature.com>], copyright 1991, Macmillan Magazines Ltd. [35].

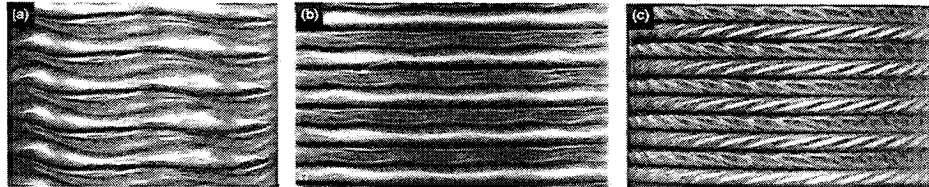


FIGURE 9. Secondary flows arising from instability of Taylor vortex flow: wavy vortex flow with waves on all vortex boundaries, (b) wavy inflow boundaries, and (c) “twisted” vortices (waves in the vortex core but not on the vortex boundaries). The flow is visualized using a dilute suspension of small flat flakes (Kalliroscope). Reprinted with permission from *J. Fluid Mech.*, Cambridge University Press [27].

symmetries. The selection rules derived from symmetry yielded only four possible states, which were just the four states found in an experiment [27]: vortices with waves on both the inflow and outflow boundaries (Fig. 9(a)), vortices with waves on only the inflow boundaries (Fig. 9(b)), vortices with waves on only the outflow boundaries (not shown), and vortices with flat inflow and outflow boundaries with waves in the vortex core (Fig. 9(c)).

Another example of use of symmetry is illustrated in Fig. 10, which shows a sequence of images of disordered surface wave patterns, where the spatial correlations extend only about one wavelength [38,39]. However, an analysis by Dellnitz et al. [40] predicted that, even though the instantaneous patterns may have no apparent order, the time-averaged patterns should exhibit the symmetry of the boundaries; the time-averaged pattern in Fig. 10 is in accord with this prediction.

For some systems there are no equations of motion or even mathematical models, and one must rely on experiment to determine what kinds of phenomena can

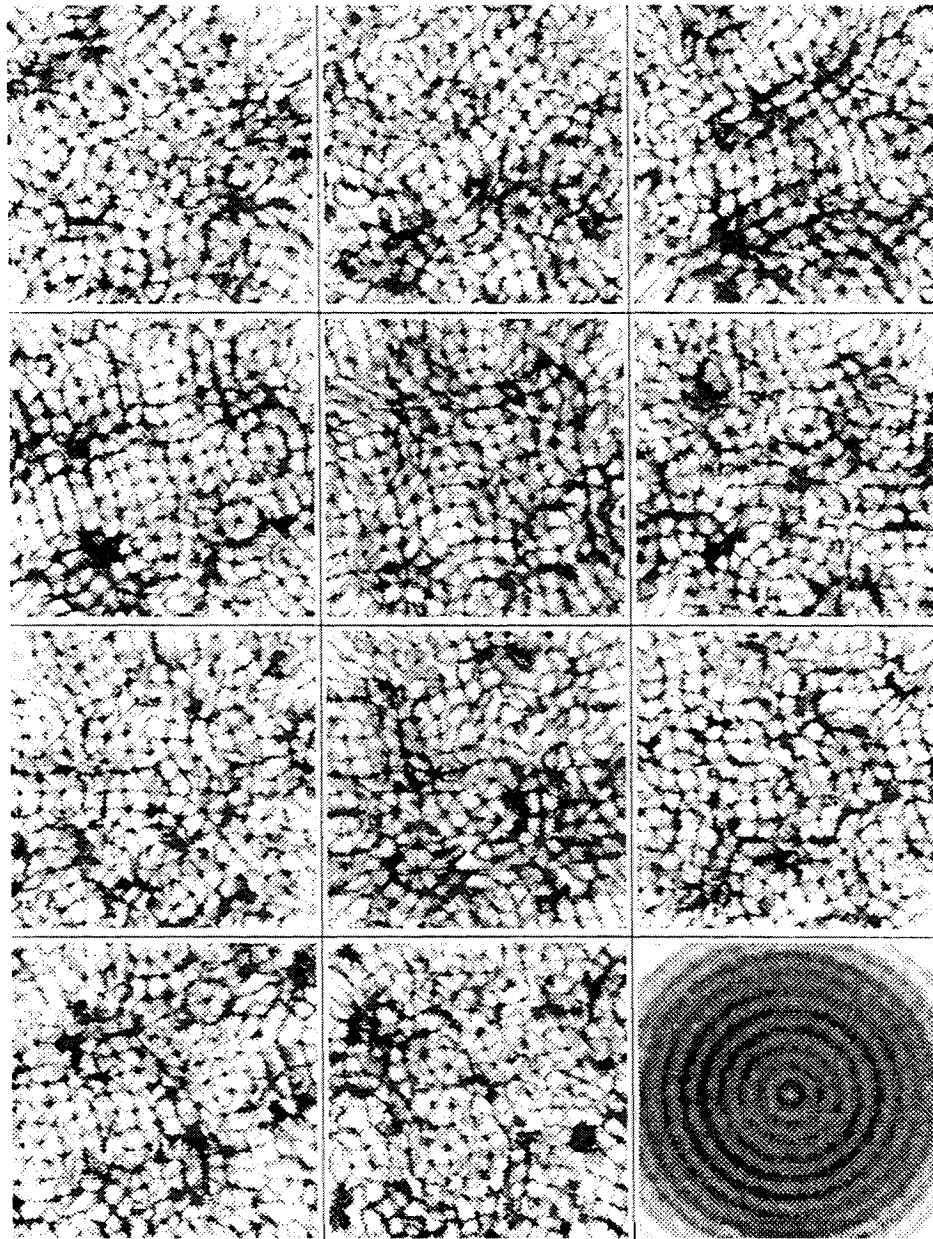


FIGURE 10. A sequence of disordered surface wave patterns observed in a vertically oscillated liquid layer. The individual pictures are snapshots, illustrating the lack of order, but the time-averaged pattern at the bottom left has the symmetry of the container. Reprinted with permission from Proc. Natl. Acad. Sci., USA, copyright 1995, National Academy of Sciences, USA [39].

occur. Vertically oscillated containers of small particles are a good example. Continuum models have successfully described some patterns observed in these systems, but thus far the models have had limited predictive value. Experiments on thin granular layers in evacuated containers, conducted as a function of the acceleration amplitude and frequency, yield a bifurcation structure every bit as rich as that in flow between concentric rotating cylinders (cf. Fig. 6)[41]-[42]. When the acceleration amplitude exceeds g , the gravitational acceleration, the layer of particles leaves the container for part of the cycle. The layer remains flat until the acceleration reaches about $2.5g$, where spatial patterns spontaneously form, squares at low frequencies and stripes at high frequencies; see Fig. 11. At higher acceleration amplitudes, hexagons and a variety of more complex patterns form. Stable, localized, standing wave structures form when the acceleration is decreased just slightly below the critical value at which patterns first form with increasing acceleration amplitude. Some of these localized structures are shown in the lower row in Fig. 11.

We have not discussed chaos or routes to chaos. Systems described by a few coupled *ordinary* differential equations are described by low dimensional phase space attractors, and these systems often exhibit bifurcation sequences that have universal properties, e.g., the period doubling route to chaos, a periodic to quasiperiodic to chaotic sequence, and intermittency [43]. However, in the spatially extended systems of interest here, low dimensional attractors and the routes to chaos are not usually observed, except for small systems (only a few characteristic wavelengths in size) not too far beyond the primary instability. Nevertheless, dynamical systems concepts such as strange attractors, fractal basin boundaries, multiplicity (multiple stable states for the same control parameters), are often helpful in interpreting the behavior of spatially extended systems, especially in the parameter range where disorder first develops as the system is driven beyond the primary instability.

PERSISTENCE OF ORDER

Very far from equilibrium ($R \gg 1$), a flow becomes turbulent, disordered in space and time and exhibiting a wide range of spatial scales. Yet a surprising degree of order often persists. Figure 12 shows turbulent Taylor vortices at a value of R nearly two orders of magnitude larger than that at which Taylor vortices first form [44]. The vortices are clearly discernible, and they are still apparent when R is increased by another order of magnitude.

The Great Red Spot of Jupiter is another example of the persistence of order in a turbulent flow. This large vortex was first observed by Robert Hooke in 1664 [45]. The width of the vortex is about twice the diameter of the earth, and typical velocities are of order 50 m/s; hence the Reynolds number is enormous. The pictures obtained by Voyager 2 in 1979 and Galileo in 1996 show that the Jovian atmosphere is strongly turbulent. There are many long-lived vortices in the eastward and westward jets in the Jovian atmosphere; the Great Red Spot is just the largest of the vortices. The earth's atmosphere is also at high Reynolds

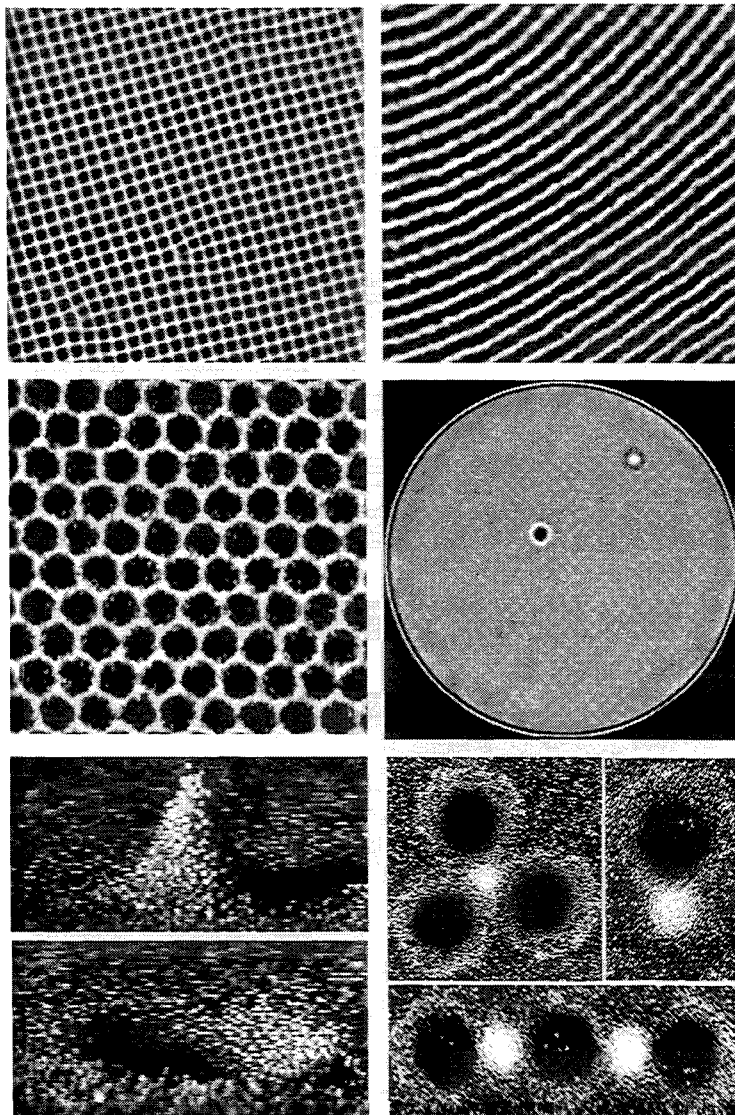


FIGURE 11. Patterns formed in a vertically oscillated thin layer of bronze spheres (0.16 mm in diameter) in a 127 mm diameter container. Top left, squares (3.2g, 20 Hz); top right, stripes (3.3g, 67 Hz); center left, hexagons (4.0g, 67 Hz); each image is 50 mm \times 50 mm [41]. The image on the right in the center row shows a layer with two localized standing wave structures (*oscillons*) of opposite phase; the white dot is seen as a peak when viewed from the side (upper image on the bottom left), while the black dot is a crater (lower image on the bottom left). The pictures on the lower right show bound states (oscillon “molecules”) — a tetramer, a dimer, and a polymer chain [42].

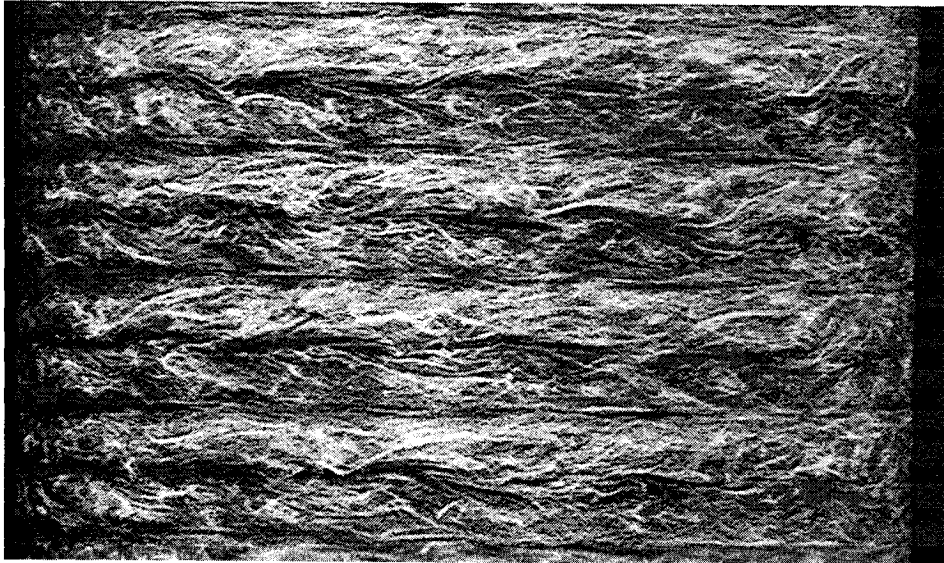


FIGURE 12. Turbulent flow between concentric cylinders with the inner cylinder rotating and the outer cylinder at rest [44]. Four vortex pairs are discernible. $R = 7600 = 92R_c$.

number. Coherent structures are readily apparent on a weather map, which shows large cyclonic low pressure vortices and anti-cyclonic high pressure vortices, and a wavy jet stream which encircles the globe in the stratosphere at middle latitudes.

The persistence of coherent vortices and jets in strongly turbulent flows can profoundly affect the transport properties of the flow. A recent experiment on a rapidly rotating flow containing jets and vortices showed that, for the case examined, the mean square displacement of tracer particles, $\langle(\delta r)^2\rangle$, did not vary linearly with time as in normal diffusive processes, rather, $\langle(\delta r)^2\rangle \propto t^\gamma$ with $\gamma = 1.6$ [46,47]. The persistent coherent structures were responsible for this “anomalous diffusion”: particles would become trapped for a while in a vortex and then escape and travel very long distances in a jet. By tracking large numbers of individual particles it was possible to determine the probability distribution function for a single step of length L . The result was $P(L) \propto L^{-\mu}$ with $\mu = 2.2$ for the case examined. Hence the mean square step size, $\langle L^2 \rangle = \int L^2 P(L) dL$, diverged and the central limit theorem could not be used to analyze the transport.

Probability distribution functions with divergent second moments were studied by Paul Lévy, starting in the 1930s, and applied to physical systems by Scher, Shlesinger, and Montroll a half century later [48]. The experiment described in the previous paragraph was the first to directly observe “Lévy flights”, which lead to a probability distribution function with a divergent second moment. The experiment was conducted on a simple isothermal flow with circularly symmetric forcing and circularly symmetric boundaries. This is a far cry from a real ocean or atmosphere,

but the persistence of order (i.e., jets and vortices) in planetary flows may lead to mixing properties rather different from those described by normal diffusive processes. In some cases the jets and vortices could lead to greatly enhanced mixing. In other cases, the persistent structures could lead to barriers to transport, perhaps analogous to the invariant curves (KAM tori) in Hamiltonian dynamical systems [49].

PROSPECTS

As we have described, the nonlinear partial differential equations governing a macroscopic system driven away from thermodynamic equilibrium can be solved for a base state, which is always stable sufficiently close to equilibrium. The stability of the base state can be determined by solving a linear equation involving an infinitesimal perturbation of the base state. At a critical control parameter value, the base state becomes unstable and spatial structure emerges with a wavelength $2\pi/k_c$, which is determined from the linear stability analysis. The form of the pattern that emerges and the development of this pattern with increasing control parameter can be determined from a weakly nonlinear perturbation analysis (“amplitude equations”).

Far beyond the primary instability, each system behaves differently. Details matter, as Langer has emphasized [50]. There is no universality. However, the situation is not bleak. While there are no universal sequences leading to complex spatiotemporal behavior, similar bifurcations and patterns are frequently found in numerical simulations of simple models and in experiments on diverse systems. Simulations, experiments, and analyses are providing concepts and tools that are broadly applicable to systems driven far from equilibrium.

The study of nonequilibrium systems is inherently interdisciplinary. The problems often cross the boundaries of the traditional disciplines of mathematics, physics, chemistry, biology, or engineering. Important mathematical questions remain open, for example, what is the fundamental difference between patterns formed in a bounded (or periodic) domain, where the differential equations have compact groups of symmetry, and patterns formed in systems where boundaries are unimportant, where the equations have noncompact symmetry groups? One general area of applications concerns the control of industrial processes, which usually operate far from thermodynamic equilibrium. To produce more product, larger gradients are imposed, thus driving a system further from equilibrium and leading to instabilities and loss of control. Methods are now being developed to control processes in far from equilibrium conditions, even on unstable states remote in phase space from the attractor for a given set of control parameters; this would be desirable in situations where the unstable state is more efficient than the stable state [51].

In closing, we raise the question of whether or not the study of the emergence of patterns in systems driven away from equilibrium is a “fundamental” problem.

It does not involve questions regarding the fundamental interactions between particles, but it does seem fundamental in the sense stated by Philip Anderson in his essay, "More is Different" [52]:

The ability to reduce everything to simple fundamental laws does not imply the ability to start from those laws and reconstruct the universe. ... at each level of complexity entire new properties appear, and the understanding of the new behaviors requires research which I think is a fundamental in its nature as any other.

ACKNOWLEDGMENTS

I gratefully acknowledge the collaboration and support of the members of the Center for Nonlinear Dynamics of the University of Texas. I also thank Jerry Gollub (Haverford College) and Marty Golubitsky (University of Houston) for many helpful discussions over the past two decades about pattern formation. My research on pattern formation has been made possible by the support of DOE, ONR, NASA, NSF, the Welch Foundation, and the University of Texas.

I thank Princeton University Press for permission to reprint this paper (with revisions and corrections) from *Critical Problems in Physics*, ed. by V. L. Fitch, D. R. Marlow, and M. A. E. Dementi, editors, Princeton University Press, 1997, Ch. 4, pp. 51-74 (including a discussion).

REFERENCES

1. Taylor, G. I., Phil. Trans. Roy. Soc. (London) **A223**, 289 (1923).
2. Bénard, H., Rev. Gen. Sci. Pure Appl. **11**, 1261 (1900).
3. Lord Rayleigh, Philos. Mag. **32**, 529 (1916).
4. Block, M. J., Nature **178**, 650 (1956); Pearson, J. R. A., J. Fluid Mech. **4**, 489 (1958).
5. Schatz, M. F., VanHook, S. J., McCormick, W. D., Swift, J. B., and Swinney, H. L., Phys. Rev. Lett. **75**, 1938 (1995).
6. Zaikin, A. N., and Zhabotinsky, A. M., Nature **225**, 535 (1970).
7. Bodenschatz, E., de Bruyn, J., Ahlers, G., and Cannell, D. S., Phys. Rev. Lett. **67**, 3078 (1991).
8. Lechleiter, J., Girard, S., Peralta, E., and Clapham, D., Science **252**, 123 (1991).
9. Jakubith, S., Rotermund, H. H., Engel, W., von Oertzen, A., and Ertl, G., Phys. Rev. Lett. **65**, 3013 (1990).
10. Glass, L., Physics Today **49**(8), 40 (1996).
11. Garfinkel, A., Spano, M. L., Ditto, W. L., Weiss, J. N., Science **257**, 1230 (1992); Garfinkel, A., et al., J. Clinical Investigation **99**, 305 (1997).
12. Gray, R. A., Jalife, J., Panifilov, A., Baxter, W. T., Cabo, C., Davidenko, J. M., and Pertsov, A. M., Circulation **91**, 2454 (1995).
13. Gollub, J. P., and Frielich, M. H., Phys. Fluids **19**, 618 (1976).

14. Cross, M. C., and Hohenberg, P. C., *Revs. Mod. Phys.* **65**, 851 (1993).
15. Ahlers, G., "Over Two Decades of Pattern Formation, a Personal Perspective" in *25 Years of Nonequilibrium Statistical Mechanics*, edited by Rubí, M., Springer, 1995.
16. Turing, A. M., *Phil. Trans. Roy. Soc. (London)* **237**, 37 (1952).
17. Ouyang, Q., and Swinney, H. L., in *Chemical Waves and Patterns*, ed. by Kapral, R., and Showalter, K., Dordrecht: Kluwer, 1995, p. 269.
18. Murray, J. D., *Mathematical Biology*, New York: Springer-Verlag, 1989.
19. Castets, V., Dulos, E., Boissonade, J., and de Kepper, P., *Phys. Rev. Lett.* **64** 2953 (1990).
20. Nosztcizius, Z., Horsthemke, W., McCormick, W. D., Swinney, H. L., and Tam, W. Y., *Nature* **329**, 619 (1987).
21. Tam, W. Y., Horsthemke, W., Nosticzius, Z., and Swinney, H. L., *J. Chem. Phys.* **88**, 3395 (1988).
22. Ouyang, Q., and Swinney, H. L., *Nature* **352**, 610 (1991).
23. Ouyang, Q., Li, R., Li, G., and Swinney, H. L., *J. Chem. Phys.* **102**, 2551 (1995).
24. Residori, S., Ramazza, P. L., Pampaloni, E., Boccaletti, S., and Arcchi, F. T., *Phys. Rev. Lett.* **76**, 1063 (1996).
25. Fine, K. S., Cass, A. C., Flynn, W. G., and Driscoll, C. F., *Phys. Rev. Lett.* **75**, 3277 (1995).
26. Fauve, S., Kumar, K., Laroche, C., Beysens, D., and Garrabos, Y., *Phys. Rev. Lett.* **68**, 3160 (1992).
27. Andereck, C. D., Liu, S. S., and Swinney, H. L., *J. Fluid Mech.* **164**, 155 (1986).
28. Dyson, F., *New York Review of Books* (May 25, 1995), p. 31.
29. Holmes, P., talk at the University of Texas, October 28, 1996.
30. Lee, K. J., McCormick, W. D., Ouyang, Q., and Swinney, H. L., *Science* **261**, 192 (1993).
31. Petrich, D. M., and Goldstein, R. E., *Phys. Rev. Lett.* **72**, 1120 (1994).
32. Hagberg, A., and Meron, E., *Phys. Rev. Lett.* **72**, 2492 (1994).
33. Pearson, J. E., *Science* **261**, 289 (1993).
34. Li, G., Ouyang, Q., and Swinney, H. L., *J. Chem. Phys.* **105**, 10830 (1996).
35. Lee, K. J., McCormick, W. D., Swinney, H. L., and Pearson, J. E., *Nature* **369**, 215 (1994).
36. Golubitsky, M., Stewart, I. N., and Schaeffer, D. G., *Singularities and Groups in Bifurcation Theory: Vol. II*, Applied Mathematical Sciences **69**, New York: Springer-Verlag, 1988; Stewart, I. N. and Golubitsky, M., *Fearful Symmetry: Is God a Geometer?*, Oxford: Blackwell Publishers, 1992.
37. Iooss, G., *J. Fluid Mech.* **173**, 273 (1986).
38. Gluckman, B. J., Marcq, P., Bridger, J., and Gollub, J. P., *Phys. Rev. Lett.* **71**, 2034 (1993).
39. Gollub, J. P., *Proc. Natl. Acad. Sci. USA* **92**, 6705 (1995).
40. Dellnitz, M., Golubitsky, M., and Melbourne, I., in *Bifurcation and Symmetry*, ed. by Allgower, E. et al., ISNM **104**, 99, Birkhauser, 1992.
41. Melo, F., Umbanhowar, P. B., and Swinney, H. L., *Phys. Rev. Lett.* **75**, 3838 (1995); Umbanhowar, P. B., Melo, F., and Swinney, H. L., *Nature* **382**, 793 (1996).
42. Umbanhowar, P. B., Ph.D. Dissertation, University of Texas at Austin, 1996.

43. Ott, E., *Chaos in Dynamical Systems*, Cambridge University Press, 1993.
44. Lathrop, D. P., Fineberg, J., and Swinney, H. L., *Phys. Rev. A* **46**, 6390 (1992).
45. Hooke, R., *Phil. Trans. Roy. Soc. (London)* **1**, 2 (1666).
46. Weeks, E. R., Urbach, J. S., and Swinney, H. L., *Physica D* **97**, 291 (1996).
47. Solomon, T. H., Weeks, E. R., and Swinney, H. L., *Physica D* **76**, 70 (1994).
48. For a review, see Klafter, J., Shlesinger, M. F., and Zumofen, G., *Physics Today* **49**(2), 33 (1996).
49. Sommeria, J., Meyers, S. D., and Swinney, H. L., *Nature* **337**, 58 (1989); Behringer, R. P., Meyers, S. D., and Swinney, H. L., *Phys. Fluids A* **3**, 1243 (1991).
50. Langer, J. "Nonequilibrium Physics," in *Critical Problems in Physics*, ed. by Fitch, V. L., Marlow, D. R., and Dementi, M. A. E., Princeton University Press, 1997, Ch. 2, pp. 11-27.
51. Control theory is a well-developed subject with an extensive literature. A dynamical systems method is used to control a remote unstable state in Petrov, V., Haaning, A., Muehlner, K. A., VanHook, S. J., and Swinney, H. L., *Phys. Rev. E* **58**, 427 (1998); see references therein for other work on control.
52. Anderson, P. W., *Science* **177**, 393 (1972).